Integrated Modelling of ITER Plasma Dynamics and Wall Processes Following Type I ELMs and Consequences for Tokamak Operation

S.E. Pestchanyi 1), V.M. Safronov 2), I.S. Landman 1), G. Janeschitz 1),
A. Loarte 3), Y. Igitkhanov 1), B.N. Bazylev 1)

1) Forschungszentrum Karlsruhe, IHM, FUSION, P.O. Box 3640, 76021 Karlsruhe, Germany
2) State Research Centre TRINITI, 142190, Moscow Region, Troitsk, Russian Federation
3) ITER Organisation, Cadarache, 13108, Saint Paul Lez Durance Cedex, France

E-mail contact of main author: serguei.pestchanyi@ihm.fzk.de

Abstract: The anticipated regime of ITER is the H-mode in which the ELMs can significantly deteriorate the operation. The lost plasma is dumped into the SOL and then impacts on the target producing sputtering and vaporization erosion. The resulting contamination of plasma core by eroded atoms can eventually cause the disruption. For tokamak modelling which accounts for the transients, the MHD code FOREV has been developed. The FOREV simulates the processes on the time scale of 1 ms with the CFC wall. The modelling for ITER plasma evolution following the carbon influxes reveals the significant impurity contamination of the edge plasma, which can cause large radiation losses and eventually leads to the collapse of the confinement at lesser ELM sizes than that determined by armour lifetime limitations. To validate the code, dedicated experiments have been carried out. CFC targets manufactured for ITER have been exposed at the plasma gun MK-200UG in TRINITI. On the basis of these experiments, significant plasma contamination is expected after ITER transients if heat deposition on target exceeds 0.5 MJ/m^2, which is above the vapourization threshold. This result agrees with the FOREV simulations.

1. Introduction

The anticipated regime of the tokamak ITER is the H-mode in which the repetitive outbreaks of the edge-localized mode (ELM) with the duration ~ 0.5 ms can significantly influence the operation. On the basis of scaling from present experiments [1,2], the ELM induced energy deposition at the divertor armour can reach up to several MJ/m^2. The lost plasma is dumped into the scrape-off layer (SOL), propagates along the magnetic field lines and impacts on the target producing surface erosion by physical sputtering and vaporization. The following contamination of core plasma by sputtered and eroded atoms can deteriorate the confinement and even cause a disruption.

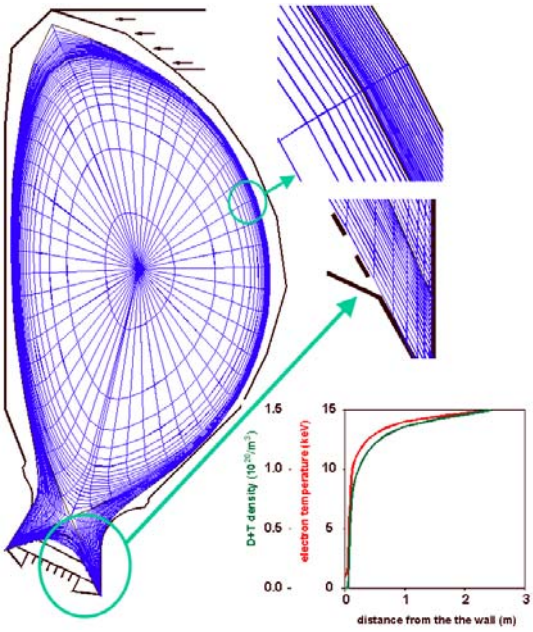

Fig. 1 FOREV calculation grid covers the core, the SOL and the private region. Initial profiles of core density and temperature (the same for all ELMs and disruption simulations) are shown.

The computer codes have been developed in FZ-Karlsruhe for the purpose of predictive modelling of transient events in ITER; analysis and validations with experiments carried out in TRINITI. Due to strong coupling between the edge plasma and diverse wall processes, the relevant modelling requires a simultaneous description of plasma transport at the edge both across and along the magnetic field lines which

terminate at the material surfaces. This allows one to establish appropriate boundary conditions for transport equation on the whole plasma region. Thus numerical algorithms valid in the whole plasma volume have to be developed. The transient particle and energy flows have to be calculated together with the transport of electromagnetic radiation.

The code FOREV (Fig. 1) developed in FZK models transient processes on the time scale of 1 ms assuming the CFC wall. It calculates the vapour shield formation in front of ITER divertor plates, screening efficiency against strong ELMs and during the disruptions and the following propagation of sputtered and eroded carbon impurities into the SOL and the edge of confined plasma. For validation of FOREV a dedicated research has been developed in frame of FZK-TRINITI collaboration. CFC targets manufactured in EU for ITER divertor armour have been exposed to pulsed magnetized hydrogen streams at the plasma gun MK-200UG, with the pulse duration 0.05 ms, ion energy 2.5 keV and in leading magnetic field up to 2.5 T [3]. Radiation properties of evaporated carbon were studied near the target surface up to the distance of 15 cm. The multiple ionization of carbon ions, their temperature, density and velocity have been measured as functions of plasma heat load.

2. Experiments at MK-200 UG and FOREV validation

The MK-200UG reproduces the energy flux, impact ion energy, plasma density and pressure of ITER ELMs, but has 10 times smaller time duration. Therefore the vaporization threshold pulse energy density, q_{vap} and the threshold of vapour shield, q_{vs} are a factor of 3 lower, than after the ITER ELMs [4]. The CFC NB31 was tested for the different heat flux magnitudes. The samples have a flat rectangular shape with a face surface 2.5×2.5 cm and the thickness 1 cm. To measure the absorbed energy, the targets are equipped by thermocouples. The surface temperature T_s is measured by a pyrometer with time resolution 0.1 μs. For analyses of evaporated carbon, visible (4000-7000A) and EUV (10-400A) spectrometers with space resolution of 0.1 cm were applied [3].

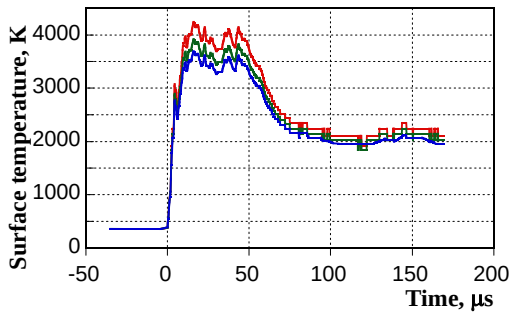

FIG. 2: Surface temperature of CFC target evaluated for surface emissivity 1 (in blue), 0.8 (green) and 0.6 (red).

For evaluation of realistic CFC thermal conductivity, λ, the threshold of CFC vaporisation has been measured and then the FOREV value of λ [4] was adjusted, to achieve the measured vaporization threshold in the simulation for MK-200UG configuration. In the experiment a weak evaporation occurs already at q ~ 0.15 MJ/m^2 ($T_s \approx 3600$ K) and intense evaporation starts at q ≈ 0.2 MJ/m^2 ($T_s \approx 4000$ K). With further increase of heat flux q, the surface temperature T_s remains unaltered, which indicates that $q_{vap} \approx 0.2$ MJ/m^2. Fig. 2 presents T_s measured by the pyrometer at q = 0.24 MJ/m^2. These measurements confirm also the vaporization threshold 0.2 MJ/m^2. At q = 0.2 – 0.3 MJ/m^2 the carbon plasma consists mainly of C^{+1} – C^{+5} ions at the temperature 10 – 30 eV. The density of C atoms near the surface is $n_C = 2\times10^{23}$ m^{-3}, and atoms propagate along the magnetic field with a velocity 1–2×10^4 m/s.

Comparison of measured and simulated surface temperature T_s for the CFC target in the case of q = 0.24 MJ/m^2 and 0.09 MJ/m^2 are shown in Fig.3. It is seen that the reference thermal conductivity λ_{ref} of NB31 brings to big discrepancy being used in calculations (the green curve in Fig. 3). However, if one assumes $\lambda \approx \lambda_{ref}/3$ for all temperatures, the agreement in the leading front shape and in maximum T_s is restored (blue line). It seems that after a hundred of severe thermal shocks the CFC get significantly degraded due to the brittle destruction on the depth of 0.1 – 0.2 mm. Therefore the contradiction is attributed to a thin surface layer of few hundred μm which is damaged by the previous impacts. As to the CFC bulk, it has $\lambda \approx \lambda_{ref}$, which is confirmed by measurements at the JUDITH facility. For stationary heating regime, the temperature drop across the damaged layer is small compared to bulk temperature drop. In this case λ_{ref} determines the thermal transport. But during the fast heating on the time scale of 0.1 ms only the pre-damaged surface layer conducts the heat, so $\lambda \approx \lambda_{ref}/3$. Thus by fitting λ a good agreement between the measured and the calculated surface temperature was finally achieved.

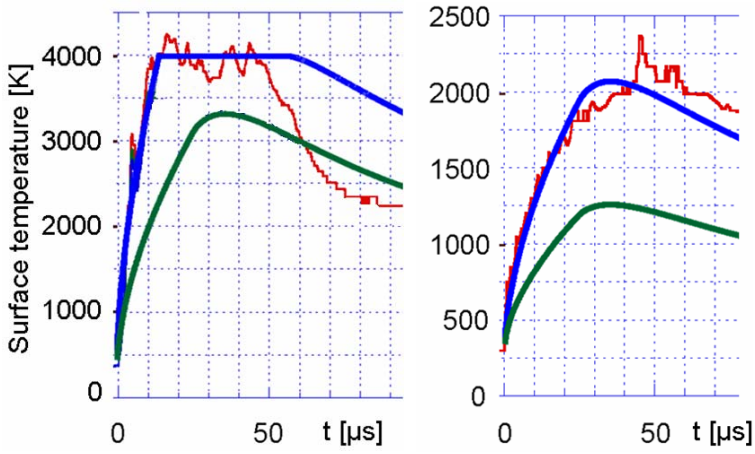

Fig. 3. Measured and simulated surface temperature T_s for q = 0.24 MJ/m^2 and 0.09 MJ/m^2 are shown. The lower numerical curve of T_s (in green) corresponds to $\lambda \approx \lambda_{ref}$ and the other (blue) to $\lambda \approx 0.35\lambda_{ref}$.

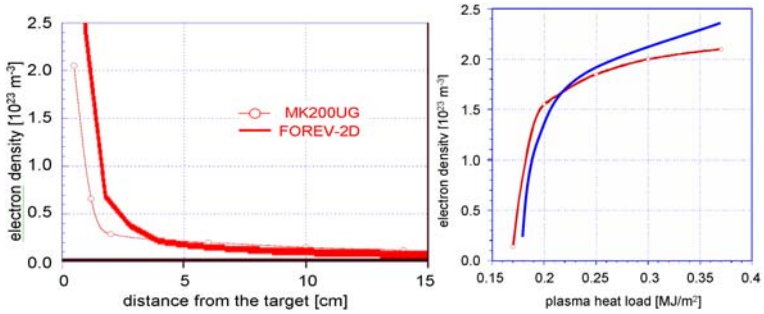

FIG. 4: Comparison of measured and simulated space distribution of electron density in front of CFC target at 10-15 μs. q = 0.3 MJ/m^2, $\lambda = 0.35\lambda_{ref}$ shown in the left panel and the density at 1-cm distance from the target versus plasma heat load.

Using the results of NB31 CFC vaporization in the MK-200UG facility, the validation between the carbon plasma parameters and the plasma transport simulated with FOREV code for ITER conditions has been completed. Two series of experiments have been performed, one with a narrow target letting plasma stream to bypass it, and another with a wide target covering whole plasma stream. In the first case and the regime with surface vaporisation the vapour shield gets thin, which increased the vapour shield threshold for approximately four times.

In the series with the wide target, the carbon density of the vapour shield in front of the target has been measured at only one time moment. Comparison of the space distribution of electron density for the measured and the simulated plasma shield densities illustrated in Fig. 4 showed good agreement. The shield densities at the distance 1 cm from the surface measured and calculated for various power heat loads in the MK-200UG facility are also in a reasonable

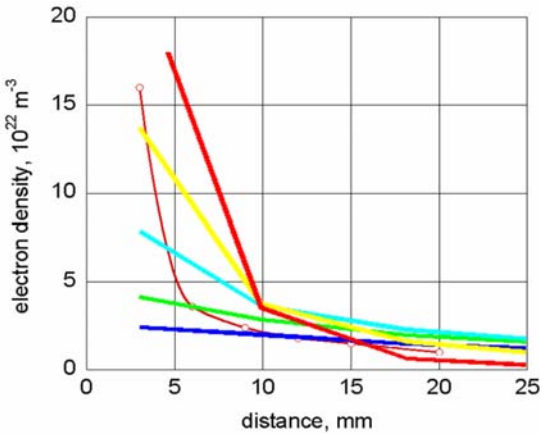

Fig. 5. The experimental curve (marked by the circles) corresponds to the time integral over whole pulse of 0.8 MJ/m^2 total heat load. The simulated curves correspond to the time moments 6, 12, 25, 31 and 38 μs.

agreement, as it is seen from the right panel in Fig. 4. Since in these experiments such measurements have not been done at different times, for rough estimation of correlation between the measurements and the simulations at different times one can use the results of second experimental series in which the integral of electron density over pulse time has been measured at different distances from the target surface. It is quite difficult to estimate the details of these measurements, but comparison of them with the corresponding calculated density distributions at several time moments may convince that there are no large differences from the experimental densities. Fig. 5 shows the measured dependence of the time integrated electron density on the distance from the target in comparison with the simulated spatial dependences.

3. FOREV modelling of plasma contamination

During disruptions and ELMs the heat flux q on the divertor surface increases drastically compared to that of the stationary regime, but the surface impact gets limited due to the carbon vapour shield that arises close to the separatrix shrike point (SSP). Fig. 6 shows the target heat loads with- and without the vapour shield for a simulated disruption. A large fraction of impacting energy is reradiated by the carbon plasma onto the structures surrounding the divertor. Carbon ions penetrate into SOL and then into the confinement region. As a consequence, the thermal energy of confined plasma is reradiated onto the first wall directly from the pedestal. In FOREV scenario simulating this process (typical initial plasma parameters in SOL are shown in Fig. 1) the loss of confinement is assumed due to a drastic increase of plasma cross-diffusion coefficient $D_\perp$, fitting its magnitude to the energy release W through the separatrix from 50 to 200 MJ for disruptions.

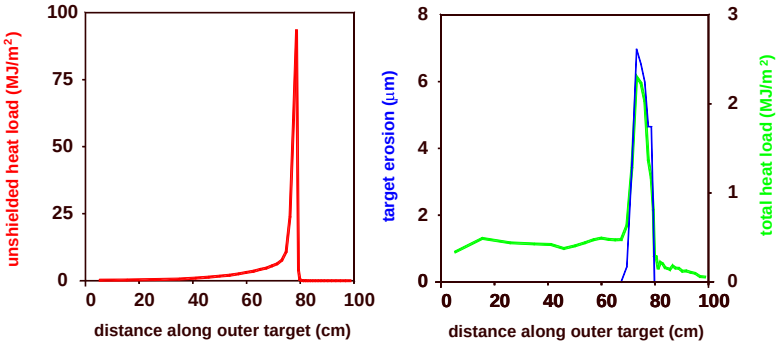

Fig. 6. Total divertor target heat loads during the disruption of 200 MJ size with- and without shielding. The profile of vaporization erosion depth is also shown.

Simulations of the tokamak thermal quench phase can be simulated in FOREV, because in this case the magnetic configuration does not change dramatically and this is inherently assumed in the code. This assumption is not valid for whole disruption, but it is adequate for thermal quench and for ELMs. The scenario used for these simulations assumes that after the ELM or disruption onset, $D_\perp$ grows linearly during 0.2 ms and then for the disruption it remains constant for 3 ms, and for ELMs it decreases exponentially with the ELM duration τ_{ELM} = 0.5 ms. It is worthwhile noting that despite of the constant $D_\perp$ during a disruption, due

to decreasing pedestal density the heat flux into the SOL across the separatrix decreases. The calculation grid of FOREV covers the plasma core and spans into SOL for different distances from the separatrix. It approaches the first wall and adjoins the divertor surface as it is shown in Fig. 1. The initial core temperature and density profiles for all simulations are also shown there. With these profiles, the large transient transport coefficients provide the required large transient fluxes of particles and energy through the separatrix and thus a large plasma density in SOL. Therefore in the simulations for both disruptions and ELMs the initial SOL plasma density and temperature are neglected. For the sake of simplicity the initial surface temperature T_s is assumed to be 1500K along all boundary of the grid, despite of the fact that in ITER the stationary T_s can be equal to this value only in a small vicinity of SSP. This rough assumption can cause only a small influence on the width of the vaporized region, because of sharp decrease of the surface heat flux with the distance from SSP.

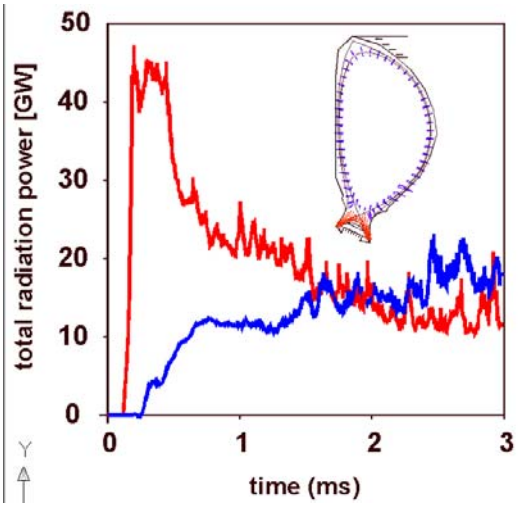

FIG. 7: Simulated radiation power from the divertor region (in red) and the core (blue) for disruption with W_{max} = 50 MJ.

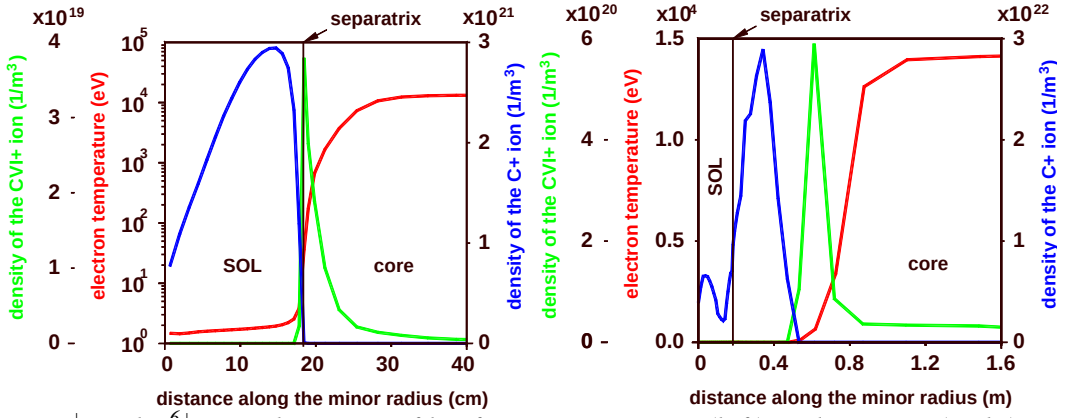

Fig. 8. C^{+} and C^{6+} ions density profiles for W_{max} = 50 MJ (left) and 200 MJ (right).

The vaporization starts from 0.06 ms (W = 200MJ) to 0.2 ms (W = 50MJ) at the SSP and takes place in a thin strip along the toroidal direction. The strip width increases according to the event size ranging typically from 5 to 15 cm for disruptions and 0 to 5 cm for the type I ELMs. The carbon plasma expanding into SOL has varying densities of 10^{21} - 10^{22} m^{-3}, which depends on the impact energy flux q. However, in case of strong ELMs and disruptions the temperature of carbon plasma near the targets depends slowly on q. It is limited by a few eV, because the heating power is immediately converted into the radiation ('radiation barrier'). As the result, the energy flux at the divertor target drops to the values less than 1 GW/m^2 (which decreases with time slightly) as long as the load can provide continuous vaporization.
Then the cold carbon plasma in SOL crosses the separatrix, mainly in a vicinity of x-point, and it also diffuses to the first wall. In the hot pedestal region, the incoming carbon plasma is almost immediately stripped up to C^{6+} state, which has limited radiation cooling rate due to the bremsstrahlung only. But with increasing the event size the carbon inflow through the separatrix can get large enough to cause fast radiation cooling of the confined plasma (MARFE). The time dependence of radiation power from the divertor region, in comparison with that from the pedestal, is shown in Fig. 7. According to the FOREV simulations, in the

case of total thermal energy W_{max} smaller than 50 MJ, radiation losses occur mainly from the divertor region. With increase of W_{max}, the losses from pedestal region become dominant.

In Fig. 8 the radial profiles of density and temperature are shown for W_{max} = 50 and 200 MJ. At W_{max} = 50 MJ the main energy is deposited at the divertor. The carbon plasma fills SOL with the density of 3×10^{21} m^{-3} and penetrates almost fully ionized into the pedestal without noticeable radiation. The main ion species is C^{6+} in the core and C^{+} in SOL, which is due to very different plasma temperatures. At W_{max} = 200 MJ the pedestal radiation losses reach 85% of these 200 MJ. In this case the pedestal plasma is eventually cooled down to a few eV and the average divertor heat load become even lower (~30 MJ) than that of the smaller disruption. The radiation cooling wave propagates in the pedestal as carbon plasma does, and pedestal thermal energy is radiated onto the first wall. The carbon plasma density in the SOL is of 3×10^{22} m^{-3}. The corresponding large diffusive inflow of carbon causes a drop of pedestal plasma temperature to few electron-volts, which in turn drastically enhances the carbon influx. The cold carbon plasma irradiates significantly due to the line radiation, and the radiation cooling wave propagates reaching the core. Fig. 8 shows the temperature and density profiles at the time moment when the cooling wave penetrates ~30 cm into the core.

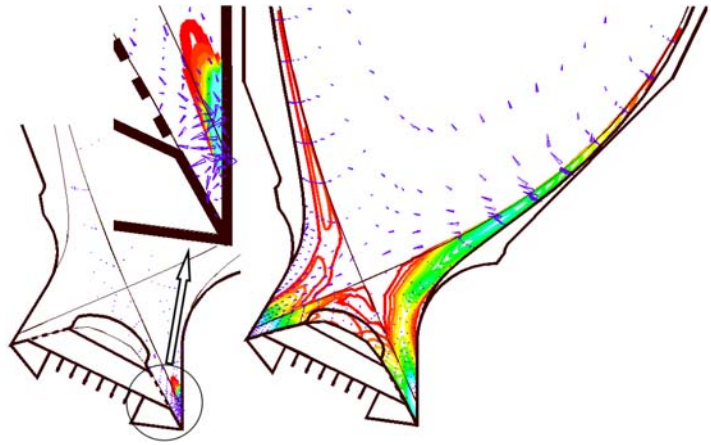

Fig.9. Carbon plasma transport during an ELM of 1.3 MJ/m^2 target heat load. The contours correspond to the density variation from 3×10^{22} m^{-3} (blue) to 2×10^{21} m^{-3} (red), the radiation heat flux is shown with arrows. The left panel shows the plasma cloud at 0.1 ms with maximum flux to the wall of 12 GW/m^2, the right one is at 0.5 ms with maximum flux of 0.3 GW/m^2.

A strong type I ITER ELMs impact is simulated in FOREV as well. Fig. 9 illustrates the propagation of vaporized carbon plasma along the magnetic field lines into SOL. After the start of vaporization the plasma shield is initially concentrated close to the target and soon the radiation heat flux to the surrounding walls becomes as large as ~10 GW/m^2. Later on the timescale 0.1 ms the carbon plasma expands into SOL and the characteristic heat load at the target becomes 30-100 times smaller, but the affected area gets much larger, gradually expanding upon the whole vessel surface.

Generally, according to the full FOREV simulations ELMs with the divertor target heat load below 1.5 MJ/m^2 size produce carbon contamination without noticeable cooling down of the pedestal plasma, and the resulting radiation load of the first wall does not cause melting of beryllium PFCs. But as simulated by FOREV, an ELM with 3.1 MJ/m^2 heat load initiates the radiation cooling wave in the pedestal, and this can terminate the confinement resulting in the disruption. The radiation heat loads in this case produce surface melting of the Be first wall close to the baffles where the heat load has maximum, however the rest region of the first wall remains not molten. The target heat fluxes and the plasma shield parameters for ELMs causing the disruption (3.1 MJ/m^2) and for the safe ELM (1.5 MJ/m^2) are shown in Fig. 10. More accurate estimation for the threshold, which runs ITER into the disruption, requires additional calculations in the range 1.5 - 3.1 MJ/m^2 of the heat load.

4. Simplified vapour shield model and vaporization erosion

FOREV simulations for ELMs have revealed that the vaporization at the divertor plate can be described in a simplified way, which saves considerably the CPU time. This model uses the fact that the plasma shield temperature is not sensitive to the heat flux. The simulations for ELMs with the shielding has shown that after the vaporization onset followed by a short transition period, the vaporization rate r_{vap} becomes almost constant during 0.15 - 0.2 ms, and r_{vap} depends only on the heat flux increase rate $\dot{G}$ of ELM. Pre-surface carbon plasma density and temperature become also approximately independent of time, which can be seen from Fig. 10. As the result, maximum vaporization depth h_{vap} after e.g. one ELM of the duration $\tau = 0.5$ ms saturates at increasing $\dot{G}$ at $h_{vap} \approx 6.5$ μm. As the vaporization area increases with increasing $\dot{G}$, the vaporized amount N_{vap} does not saturate. These details are shown in Fig. 11. The following analytical formula fits well the calculated dependence of r_{vap} on $\dot{G}$:

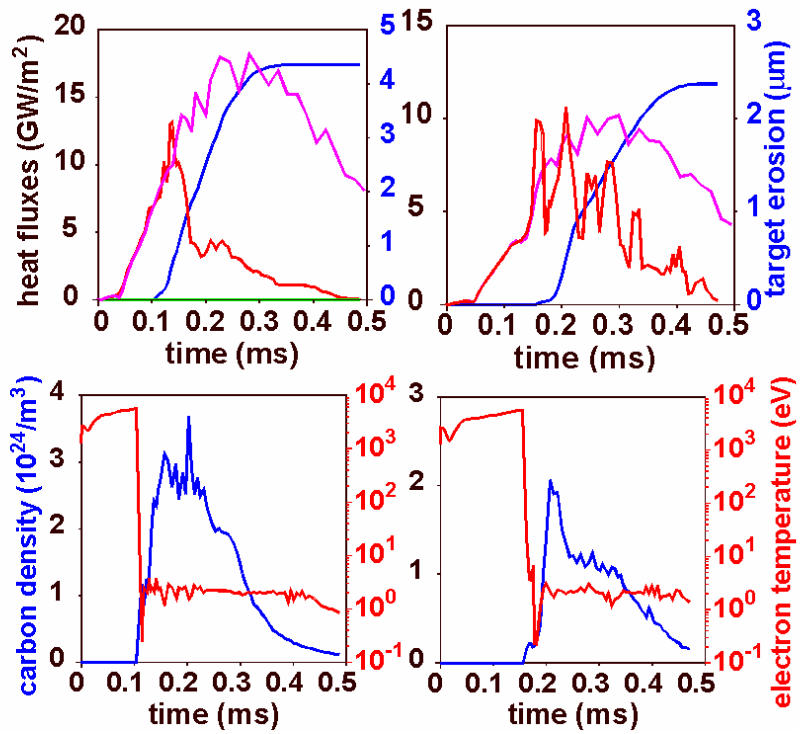

Fig.10. Upper panels show the time dependences for the heat flux to the divertor armour without (magenta curve) and with (red) the shielding and for the erosion (blue) for the ELMs of the peak heat loads of 3.1 MJ/m², and 1.5 MJ/m². The lover panels show calculated time dependences for the shield plasma temperature and density close to the target.

$$r_{vap}\left[\text{atom}/m^2 s\right] = 1.5\cdot 10^{27}\ln\left(\dot{G}/\dot{G}_0\right), \quad \dot{G} \geq \dot{G}_0, \quad \dot{G}_0 = 0.15\times 10^5\ \text{GW/m}^2\text{/s}$$

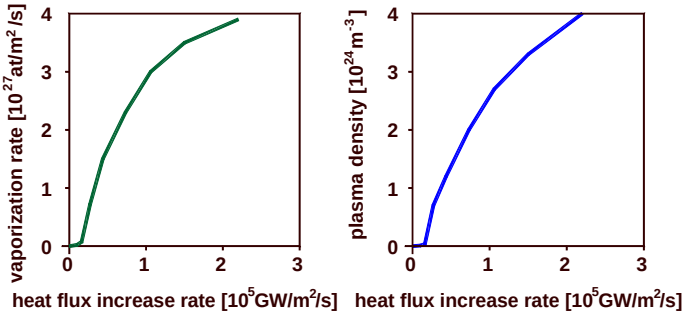

Fig. 11. Carbon vaporization rate and the plasma shield density dependence on the heat flux increase rate $\dot{G}$ for the ELMs of 0.5 ms.

As an example, at the ELM deposition energy 1.8 MJ/m^2, which corresponds to $\dot{G} = 0.27\times 10^5$ GW/m^2/s and $\tau = 0.5$ ms, evaporated amount follows as $N_{vap} = 0.88\times 10^{23}$ m^{-2}.

5. Conclusions

A good agreement between the measured and the calculated by FOREV dependences of the plasma shield density on the incident heat load provide reliable validation of the carbon plasma shield simulation. High carbon plasma shield densities of 10^{23}-10^{24} m^{-3} predicted in the simulations for ELM-produced shields has been proved in MK-200UG experiments. On the basis of these experiments and simulations, significant erosion of the CFC divertor armour is expected during ITER transients at the target heat deposition above 0.5 MJ/m^2, which corresponds to the vaporization threshold. The erosion at 0.8 MJ/m^2, is ~1 μm per ELM, which is intolerable.

FOREV simulations have revealed that type I ELM of 3.1 MJ/m^2 divertor target heat load can run the confinement into the disruption due to the pedestal contamination with carbon vaporized from the divertor targets, the ELM of 1.5 MJ/m^2 load produces carbon contamination, but the core plasma survives and the loads below 0.5 MJ/m^2 are safe. Simulation of disruptions has revealed that the armour erosion is tolerable; for all the disruption sizes it is less than 10 μm per disruption. Moreover, the larger the disruption the more effective the armour shielding and the eroded material can reradiate up to 85% of the disruption energy directly from the pedestal to the first wall. For large disruptions the radiation from pedestal due to carbon influx causes beryllium first wall melting, but it occurs only close to the baffles, where the heat load is maximal. These numbers are valid only for the CFC divertor armour.

In the case of tungsten armour the tolerable ELM energy will be estimated in FOREV by taking into account the physical sputtering as a main erosion mechanism and the cleaning effect of ELMs, removing impurities from the plasma. The calculations based on the balance of the in- and outgoing impurity fluxes will help to define the tolerable ELM size.

Acknowledgements

This report was prepared as an account of work by or for the ITER Organization. The Members of the Organization are the People's Republic of China, the European Atomic Energy Community, the Republic of India, Japan, the Republic of Korea, the Russian Federation, and the United States of America. The views and opinions expressed herein do not necessarily reflect those of the Members or any agency thereof. Dissemination of the information in this paper is governed by the applicable terms of the ITER Joint Implementation Agreement.

References

[1] FEDERICI, G., et al, Plasma Phys. Control. Fusion 45 (2003) 1523.
[2] LOARTE, A., et al., Proc. 20th IAEA Conference, 2004 Vilamoura Portugal.
[3] SAFRONOV V.M. et al., “Evaporation and vapor shielding of CFC targets exposed to plasma heat fluxes relevant to ITER ELMs”, 13th Intern. Conf. on Fusion Reactor Materials, Nice, France, Dec. 2007, to be published in J. Nucl. Mat.
[4] PESTCHANYI S., LANDMAN I.S., “Simulation of carbon plasma shielding efficiency during ELMs”, 18th Plasma Surface Interaction Conference, Toledo, Spain, May 2008, paper P1-97.